THE JOURNAL OF BIOLOGICAL CHEMISTRY VOL. 286, NO. 10, pp. 8493–8506, March 11, 2011


# Loss of Caspase-2-dependent Apoptosis Induces Autophagy after Mitochondrial Oxidative Stress in Primary Cultures of Young Adult Cortical Neurons*[S]

Received for publication, July 14, 2010, and in revised form, January 6, 2011 Published, JBC Papers in Press, January 7, 2011, DOI 10.1074/jbc.M110.163824

**Meenakshi Tiwari, Marisa Lopez-Cruzan, William W. Morgan, and Brian Herman**[1]

*From the Department of Cellular and Structural Biology, University of Texas Health Science Center, San Antonio, Texas 78229*

**Mitochondrial dysfunctions have been associated with neuronal apoptosis and are characteristic of neurodegenerative conditions. Caspases play a central role in apoptosis; however, their involvement in mitochondrial dysfunction-induced neuronal apoptosis remains elusive. In the present report using rotenone, a complex I inhibitor that causes mitochondrial dysfunction, we determined the initiator caspase and its role in cell death in primary cultures of cortical neurons from young adult mice (1–2 months old). By pretreating the cells with a cell-permeable, biotinylated pan-caspase inhibitor that irreversibly binds to and traps the active caspase, we identified caspase-2 as an initiator caspase activated in rotenone-treated primary neurons. Loss of caspase-2 inhibited rotenone-induced apoptosis; however, these neurons underwent a delayed cell death by necrosis. We further found that caspase-2 acts upstream of mitochondria to mediate rotenone-induced apoptosis in neurons. The loss of caspase-2 significantly inhibited rotenone-induced activation of Bid and Bax and the release of cytochrome *c* and apoptosis inducing factor from mitochondria. Rotenone-induced downstream activation of caspase-3 and caspase-9 were also inhibited in the neurons lacking caspase-2. Autophagy was enhanced in caspase-2 knock-out neurons after rotenone treatment, and this response was important in prolonging neuronal survival. In summary, the present study identifies a novel function of caspase-2 in mitochondrial oxidative stress-induced apoptosis in neurons cultured from young adult mice.**

Mitochondrial dysfunction due to mutations or exposure to toxic agents leads to cellular abnormalities, including decreased ATP synthesis and increased generation of reactive oxygen species (ROS)[2] that may result in cell death (1). There is strong evidence suggesting that mitochondrial dysfunction plays an important role in neurodegeneration and neuronal death in conditions like Alzheimer disease, Parkinson disease, amyotrophic lateral sclerosis, and Huntington disease (1–3). As a result of these neurodegenerative insults, a major portion of the affected neurons dies through a process known as apoptosis (4). Apoptosis is the programmed cell death pathway mainly executed by cysteine proteases known as caspases. The apoptotic cascade of caspases is initiated by the activation of apical (initiator) caspases that include caspase-2, caspase-8, caspase-9, and caspase-10 (5–7). In response to noxious stimuli and related cellular stress situations, initiator caspases directly or indirectly activate executioner caspases, which in turn orchestrate apoptotic cell death (8). Although a growing amount of evidence suggests that caspase-mediated apoptosis contributes to neuronal cell death in a variety of neurodegenerative conditions, the identification of the caspases that initiate this response remain elusive (9, 10). Furthermore, a role for autophagy has also been identified in neurons during neurodegenerative disorders. Although autophagy generally prevents neuronal cell death, whether it plays a protective or detrimental role in neurodegenerative disease depends on the environment (11).

To gain insight into the mechanisms of neuronal death, selective neurotoxins have been identified that can cause mitochondrial dysfunction and, thus, create cellular and animal models of neurodegeneration. One of the most widely used neurotoxins is rotenone, which inhibits complex I in the mitochondrial oxidative phosphorylation pathway (12, 13). Complex I inhibition results in a decrease in ATP synthesis and an accumulation of oxidative radicals, causing detrimental oxidative stress and cell death (13–15). The mechanism of mitochondrial oxidative stress-induced cell death is well studied in embryonic neurons or cells of non-nervous tissue origin (16–20). However, it remains to be determined whether and how post-mitotic neurons are affected by mitochondrial oxidative stress-inducing agents. The existing evidence suggests that cell death in post-mitotic neurons involve different pathways than those used by embryonic neurons or the cells of other origin (21). To determine therapeutic approaches for neurodegenerative diseases, it is important to gain a better understanding of the cell death mechanisms induced in well differentiated neurons. Thus, in the present study we cultured neurons from young adult mice and used them as a model to study the mechanism of cell death induced by mitochondrial dysfunction-causing agent, rotenone. Using a technique that traps the initiator caspases *in situ*, we identified caspase-2 as the initiator caspase that acted upstream of mitochondria to mediate rotenone-induced apoptosis in neurons. Loss of caspase-2 inhibited rotenone-induced apoptosis. Inhibition of apoptosis was asso-

* This work was supported, in whole or in part, by National Institutes of Health Grant 5 R37 AG007218-21.

[S] The on-line version of this article (available at http://www.jbc.org) contains supplemental Figs. 1–5.

[1] To whom correspondence should be addressed: 7703 Floyd Curl Dr., San Antonio, TX 78229-3900. Fax: 210-567-3803; E-mail: hermanb@uthscsa.edu.

[2] The abbreviations used are: ROS, reactive oxygen species; NAC, *N*-acetylcysteine; PI, propidium iodide; AIF, apoptosis inducing factor; b-VAD-fmk, biotin-Val-Ala-Asp(OMe)-fluoromethyl ketone; *casp2*$^{-/-}$, caspase-2 knock-out; MEF, mouse embryonic fibroblast; LSM, laser scanning confocal microscope; WCL, whole cell lysates; MOMP, mitochondrial outer membrane permeabilization.

ciated with increased autophagy in rotenone-treated neurons lacking caspase-2, which was associated with an increased survival. Thus, the present study identifies a novel function of caspase-2 in mitochondrial oxidative stress-induced apoptosis in neurons cultured from young mice.

## EXPERIMENTAL PROCEDURES

*Reagents*—Glutamine, B27 supplement, fibroblast growth factor-2, penicillin/streptomycin, and Neurobasal A media were purchased from Invitrogen. Hibernate A was from BrainBits (LLC). Laminin, OptiPrep 1.32, papain, poly-D-lysine, rotenone, *N*-acetylcysteine (NAC), and trypan blue were purchased from Sigma. Pepstatin A, 3-methyladenine, bafilomycin A1, and E-64d were from Calbiochem. AlexaFluor 488 or Alexa Fluor 568 IgG secondary antibody, Calcein-AM, MitoSOX Red, Hoechst 33258, propidium iodide (PI), LysoTracker Red, and MitoTracker Red $CMH_2$xROS were purchased from Molecular Probes Inc. (Eugene, OR). Vectashield mounting medium was from Vector Laboratories, Inc (Burlingame, CA). The BCA protein assay kit and chemiluminescence system were from Pierce. $\beta$-Actin antibody, radioimmune precipitation assay buffer, and HRP-labeled anti-mouse or anti-rabbit IgG secondary antibodies were from Santa Cruz Biotechnology (Santa Cruz, CA). Antibodies against cytochrome *c* and Beclin1 were from BD Pharmingen™ (BD Pharmingen). Anti-Bax antibody (6A7 mouse monoclonal), Bid, and acetyl-CoA carboxylase were from Abcam (Cambridge, MA). Primary antibodies for apoptosis inducing factor (AIF), glyceraldehyde 3-phosphate dehydrogenase, LC3, caspase-9, caspase-3, and active caspase-3 were from Cell Signaling (Cell Signaling Technology, Danvers, MA). Biotin-Val-Ala-Asp(OMe)-fluoromethyl ketone (b-VAD-fmk) was from Enzyme Systems Products (Livermore, CA), and streptavidin-agarose beads were from Invitrogen. Caspase-2 monoclonal antibody (clone 11B4) was from Alexis Biochemicals (San Diego, CA). In case the source is not mentioned, the chemicals were purchased from Sigma. All the cell culture plastic and glassware were from Nunc (Nalgene Nunc International, Rochester, NY).

*Mice*—The caspase-2 knock-out ($casp2^{-/-}$) mice were originally generated by Dr. Junying Yuan of Harvard University and kindly provided by Dr. Carol Troy of Columbia University with the consent of Dr. Yuan (22). The mice were backcrossed with C57Bl/6 for 10 generations. The mice were housed in microisolator-topped cages and maintained in a pathogen-free environment at the Assessment and Accreditation of Laboratory Animal Care-accredited University of Texas Health Science Center-San Antonio animal facility following the NIH Guidelines for the Care and Use of Laboratory Animals. The University Institutional Animal Care and Use Committee approved the protocols used in this study. The wild type (wt) and $casp2^{-/-}$ animals were maintained in an animal room with controlled temperature and exposed to a 12:12 light-dark lighting regimen with the lights on daily from 06:00 to 18:00. Food was available *ad libitum*.

*Primary Culture of Cortical Neurons*—Cultures of cortical neurons were established from young adult mice that were 1–2 months old following the protocol published by Brewer and Torricelli (23). Briefly, the brains of the mice were dissected to isolate cortices that were transferred to 4 °C in Hibernate A supplemented with B27. Cortices were diced (0.5 mm thick) and then incubated in media containing papain (12 mg/6 ml in Hibernate A) at 30 °C in a shaker for 30 min. The digested tissue was washed free of papain and triturated 12–15 times using a siliconized Pasteur pipette. The triturated tissues were applied on the top of an OptiPrep 1.32 gradient and centrifuged at $800 \times g$ for 10 min. Debris above 4 ml was discarded, and the fractions containing neurons (fractions 2 and 3) were collected and diluted in 5 ml of Hibernate A/B27. After centrifugation at $200 \times g$ for 2 min, the resulting pellets were resuspended in 3 ml of conditional medium (Neurobasal A/B27, 0.5 mM glutamine, 10 ng/ml fibroblast growth factor-2 and penicillin/streptomycin), and viability was determined by trypan blue exclusion. For cell plating, glass coverslips in 24 multi-well plates were coated with 100 $\mu$g/ml poly-D-lysine and laminin. Approximately, $1.25 \times 10^4$ cells were plated on each 15-mm glass coverslip and allowed to attach and attain morphology. Purity of neuronal cultures was determined by staining with NeuN antibody or MAP antibody (neuron-specific) and GFAP antibody (astrocyte-specific). The cultures stained >92% for neuronal cell types after 4–7 days of culture (data not shown). Drug treatments were initiated after 5 or 6 days *in vitro*. For the treatments, the B27 supplement was replaced with B27 lacking antioxidants. Rotenone was added directly to the conditional medium and was not washed out until the end of the experiment. The control neurons were treated with similar amounts of the DMSO (rotenone carrier).

*Culture of Mouse Embryonic Fibroblasts (MEFs)*—wt, $bax^{-/-}$, $bak^{-/-}$, $bax^{-/-}$ $bak^{-/-}$, and $casp2^{-/-}$ MEFs were grown in Dulbecco's modified Eagle's medium supplemented with 10% FBS, 100 units/ml penicillin, and 100 $\mu$g/ml streptomycin.

*Neuronal Viability and Apoptosis Assay*—To determine neuronal survival, neurons were stained with Calcein-AM (2 $\mu$M) and PI (25 $\mu$g/ml) for 30 min, and the fraction of live (Calcein-AM-positive) and dead (PI) cells was determined. Hoechst 33258 staining (10 $\mu$g/ml) was performed for 30 min to visualize the nuclei. Based on nuclear morphology, cells showing apoptotic features (nuclear condensation or nuclear fragmentation) were scored. Neurons were visualized on a laser-scanning confocal microscope (LSM) (FV1000; Olympus, Tokyo, Japan), and images were captured at 40× magnification. Images were scored by an observer blind to treatment, and a minimum of 200 cells was analyzed per group in triplicate.

*Measurements of Mitochondrial Superoxide*—Mitochondrial superoxide levels were determined using MitoSOX Red (500 nM). Cortical neurons were cultured on coverslip-bottom chamber slides and maintained in Neurobasal A media supplemented with B27 for 6 days *in vitro*. Cultures were then washed with Krebs-Ringer buffer and incubated for 1 h at 37 °C with either vehicle or rotenone (20 min after MitoSOX Red loading). Subsequently, neurons were rinsed three times with warm Krebs-Ringer buffer and immediately visualized on LSM (FV1000; Olympus). Images were acquired using a 563-nm He-Ne laser to excite MitoSOX Red fluorescence. All images were scanned using 60× magnifications and using the same parameters such as laser power, detector gain, offset, pinhole,

and zoom to maintain standardized imaging conditions. Analysis of fluorescence data was performed with Image J (Windows version; National Institutes of Health). An appropriate threshold was employed to eliminate background signal in the images before histogram analysis.

*Immunofluorescence Staining for Cytochrome c, AIF, Bax, Active Caspase-3, and LC3*—To visualize mitochondria or lysosomes, live neurons were stained with MitoTracker Red (250 nM) or LysoTracker Red (500 nM) for 30 min and were washed free of dye before fixation. The neurons were fixed by the addition of 3.7% paraformaldehyde for 20 min at room temperature. Cells were washed, permeabilized (0.3% Triton X-100), blocked in 1% BSA for 1 h at room temperature, and immunolabeled with the primary antibody (1:200 dilution and overnight incubation at 4 °C). Neurons were then washed with PBS and incubated for 2 h with AlexaFluor 488 or Alexa Fluor 568 IgG secondary antibody (1:1000 dilution) at room temperature. For nuclear staining, Hoechst 33258 (10 $\mu$g/ml) was added along with the secondary antibody. Cells were washed with PBS and then with water. The coverslips were mounted with Vectashield mounting medium and sealed. Approximately, 150–200 neurons per coverslip were visualized on LSM (Olympus FV1000), and images were digitally captured and scored blindly. Each experiment was repeated at least three times with separate batches of neuronal cultures.

*In situ Labeling of Active Caspases*—To capture the active initiator caspase, neurons were pretreated with cell-permeable b-VAD-fmk (50 $\mu$M) for 2 h in the conditional media. Rotenone was then added to the neuronal cultures, and samples were collected at selected time points. To study the total active caspases, the neurons were treated with rotenone for 36 h and were incubated for 2 h with b-VAD-fmk (50 $\mu$M) before harvest. The neurons were pelleted and lysed by freeze-thawing (5–6 times) in 500 $\mu$l of CHAPS lysis buffer (150 mM KCl, 50 mM HEPES, 0.1% CHAPS, and 0.1% Nonidet P-40 with pH 7.4 also containing the protease inhibitors (2 $\mu$g/ml) and phenylmethylsulfonyl fluoride). After centrifugation at 15,000 $\times$ *g* for 10 min, the supernatant was collected, and the b-VAD-fmk-bound active caspases were captured on 30 $\mu$l of streptavidin-conjugated agarose beads. After overnight rotation at 4 °C, the agarose beads were extensively washed in lysis buffer. The biotinylated proteins were eluted from the beads by the addition of SDS sample buffer and incubated at 95 °C for 10 min. Whole cell lysates (WCL) (25 $\mu$g) that did not go through streptavidin precipitation or the eluted biotinylated proteins (25 $\mu$l) were used for SDS-PAGE and subsequent Western blotting. The endogenously biotinylated protein acetyl-CoA carboxylase functioned as a control for both pulldown efficiency and loading.

*Western Blotting*—Protein samples were separated on 4–12% gradient SDS-PAGE and transferred to PVDF membranes. The membranes were blocked in 5% skim milk for 1 h and probed overnight at 4 °C with primary antibodies in 1% skim milk or BSA. The membranes were washed and incubated for 1 h with appropriate HRP-conjugated secondary antibodies. Blots were washed and developed by using an enhanced chemiluminescence system according to manufacturer's instructions and exposed to Hyperfilm-ECL (Amersham Biosciences). The same blots were reprobed with $\beta$-actin or GAPDH or $\beta$-tubulin antibody as a loading control (no change in $\beta$-actin or GAPDH or $\beta$-tubulin protein levels was seen after treatment). Densitometry analysis band intensity was performed using Image J software.

*Data Analysis*—Data in graphs are reported as $\pm$S.E. and depict the average of at least three independent experiments. Morphological images are representative of at least three independent experiments with similar results. Statistical analysis was performed by Student's paired *t* test or a one-way analysis of variance followed by a Bonferroni post test when appropriate ($p < 0.05$ was considered significant).

## RESULTS

*Rotenone Induces Apoptosis in Cultures of Cortical Neurons from Young Adult Mice*—The dose-dependent effects of rotenone treatment have not been studied in cultures of cortical neurons obtained from young adult mice. Thus, we first determined the dose-dependent cytotoxic effect of rotenone in neuronal cultures from young adult mice. The neurons were treated with different concentrations of rotenone (0.01–1 $\mu$M) for 36 h, and viability was determined by staining neurons with Calcein-AM and PI (Fig. 1*A*). Rotenone induced a dose-dependent increase in neuronal death, and 0.3 $\mu$M rotenone, which resulted in about 48% neuronal death, was used for further experiments. Time course studies showed that rotenone induced changes in neuronal morphology within 4 h of treatment, and the fraction of dead cells began to increase after 16 h (~29%) and continued to rise over the next 72 h (see Fig. 3*B*). To identify the mode of cell death, the nuclei were stained with Hoechst 33258. We observed that rotenone treatment induced apoptosis in neurons that was characterized by chromatin condensation and/or nuclear fragmentation (Fig. 1, *B* and *C*).

*Caspase-2 Is the Initiator Caspase Activated during Rotenone-induced Apoptosis*—Because caspases are the major executioners of apoptosis, we determined which caspase acts as an initiator caspase in rotenone-treated cortical neurons. Caspase-2, caspase-8, and caspase-9 are the known initiator caspases (5–7), and the type of cellular stress determines which caspase acts as the initiator in the apoptotic process (24). To identify the initiator caspase, we employed the *in situ* trapping approach (6). Using a biotinylated form of the caspase inhibitor (b-VAD-fmk) that binds irreversibly to activated caspase, active caspase can be isolated from cell lysates and other *in vitro* preparations with the use of streptavidin (25). Incubation of the cells with b-VAD-fmk before rotenone treatment leads to trapping of the active initiator caspase and also prevents the activation of the downstream caspases. Therefore, the caspase bound to the biotinylated caspases inhibitor can be identified as the initiator caspase. We treated neurons with b-VAD-fmk (50 $\mu$M) for 2 h before adding rotenone. After rotenone treatment, neurons were harvested at different times; the initiator caspase was precipitated using streptavidin. Western blotting was performed to identify the bound caspase by probing the membranes with known initiator caspase antibodies, *i.e.* anti-caspase-2, caspase-8, and caspase-9 antibodies; the results are shown in Fig. 2*A*, and the WCL that did not undergo streptavidin capture are shown in Fig. 2*B* for comparison. The addition of b-VAD-fmk inhibited the apoptotic nuclear mor-

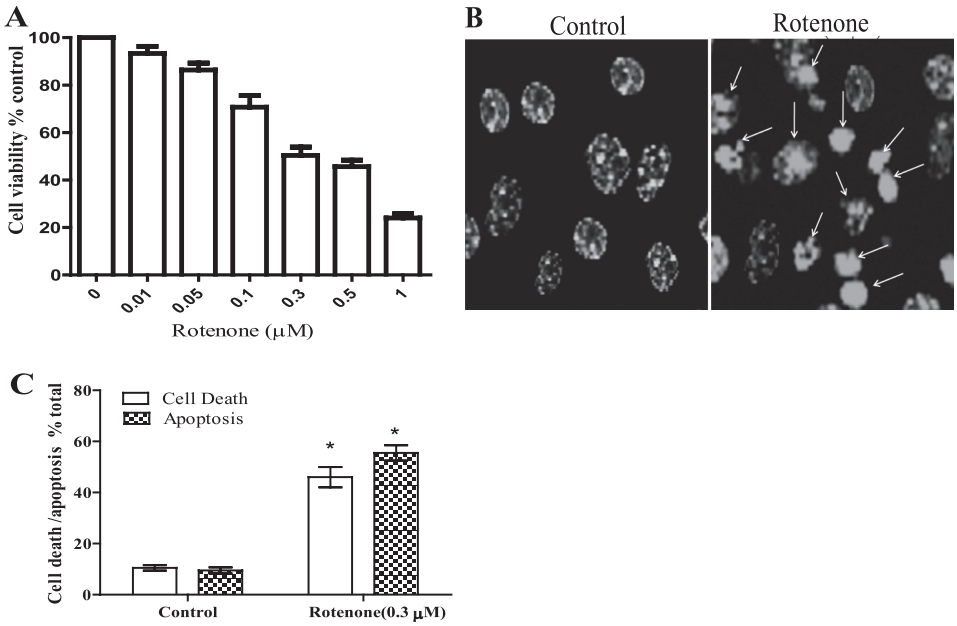


FIGURE 1. **Rotenone induces apoptotic cell death in neurons.** *A*, primary cortical neurons were treated with rotenone (0.01–1 $\mu$M) for 36 h. Cell viability was determined by counting the live cells stained with Calcein-AM and dead cells with PI. *B*, shown are representative images of Hoechst 33258-stained nuclei. *Arrows* indicate apoptosis induction after rotenone treatment. Shown are representative LSM images 40×, 3 times digital zoom. *C*, shown is a histogram representing % apoptotic cells (nuclei showing condensation or fragmentation were considered apoptotic) compared with % of cell death (PI-stained, unstained with Calcein-AM). Data (mean ± S.E., $n$ = 150–200) were derived from three separate experiments using different batches of cortical neurons.

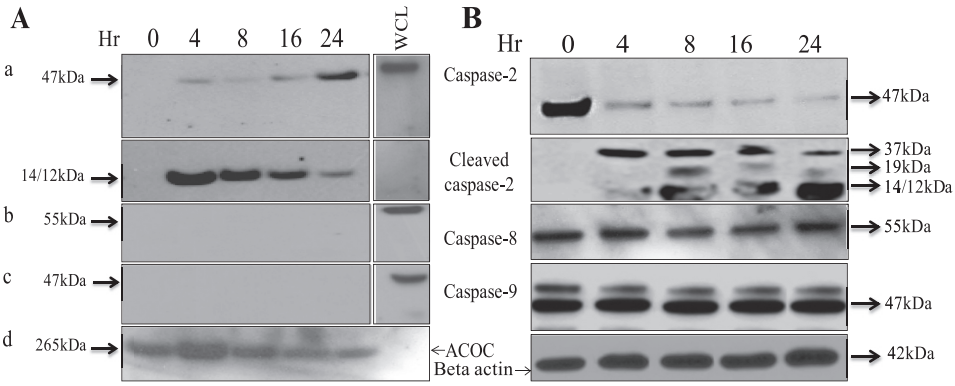


FIGURE 2. **Caspase-2 is the initiator caspase in rotenone-treated primary cortical neurons.** *A* and *B*, to identify the initiator caspase, neurons (~1 × $10^7$) were preincubated with 50 $\mu$M b-VAD-fmk for 2 h, then treated with rotenone (0.3 $\mu$M) for the indicated times. Lysates were either subjected to a streptavidin pulldown assay (*A*), or WCL were prepared (*B*), and Western blotting was performed by standard procedures for caspase-2, caspase-9 and caspase-8 using respective antibodies. WCL of untreated neurons that were not subjected to streptavidin pulldown assay acted as a positive control for immunoblotting in the streptavidin pulldown assay. The same blots were subsequently probed, and acetyl-CoA carboxylase (*ACOC*) (and loading of biotinylated proteins) or $\beta$-actin (for WCL) was used as a control for protein loading. Experiments were repeated three times, and representative blots with similar results are shown.

phology that was induced by rotenone treatment (data not shown). The results demonstrate that caspase-2 was pulled down by streptavidin precipitation within hours of the initiation of treatment, suggesting its function as the initiator caspase. Interestingly, besides observing the 47/49-kDa form that was expected during the early hours of rotenone treatment, the 12/14-kDa-cleaved form of caspase-2 was also identified. However, with more extended time, an increase in the 47/49-kDa form of caspase-2 was observed, indicating its activation (Fig. 2*Aa*). It was interesting to note that even in the WCL, within early hours of rotenone treatment the proform of caspase-2 was cleaved with the appearance of the different cleaved forms that increased further with time (Fig. 2*B*). We did not detect caspase-8a/b forms (55/57 kDa) or caspase-9 (Fig. 2*A*, *b* and *c*) in our immunoblots (performed on streptavidin pulldown samples) even after a longer time of exposure that also corroborated with WCL where no cleavage or reduction in the proform of caspase-8 or caspase-9 was observed (Fig. 2*B*), suggesting that these caspases are not the initiators during rotenone-induced apoptosis in neurons. By contrast, the specific engagement of caspase-8 or caspase-9 was observed in primary activated neurons pretreated with b-VAD-fmk and subjected to anti-Fas treatment or staurosporin, respectively (supplemental Fig. 1). Thus, our results identify caspase-2 as an initiator caspase in rotenone-induced apoptosis in primary cortical neurons.

*Loss of Caspase-2 Inhibits Rotenone-induced Apoptotic Cell Death*—Next, we determined whether caspase-2 contributes to rotenone-induced neuronal apoptosis. To avoid potential problems associated with transfection and knockdown using

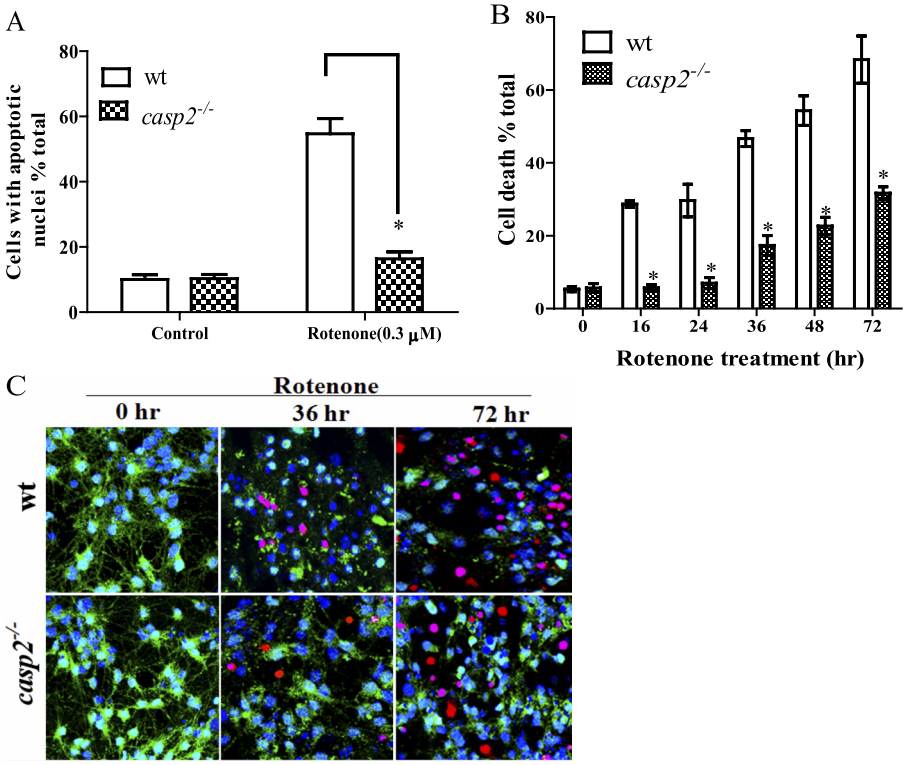


FIGURE 3. **Caspase-2 is essential for rotenone-induced neuronal apoptosis.** *A*, cortical neurons cultured from wt and *casp2*$^{-/-}$ mice were treated with rotenone (0.3 $\mu$M) for 36 h. Apoptotic cells were determined on the basis of nuclear morphology visualized by Hoechst 33258 staining. *B*, cell viability was determined by staining live cells with Calcein-AM and dead cells with PI. The time course of rotenone treatment (0.3 $\mu$M) shows cell death % control in wt and *casp2*$^{-/-}$ cortical neurons at different time points. Data (mean ± S.E., $n = 150–200$ neurons) were derived from three independent experiments with different batches of cortical neurons. *Asterisks* indicate a significant change (protection) comparing wt *versus casp2*$^{-/-}$ cortical neurons (*, $p < 0.05$). *C*, representative images of neurons treated with rotenone for 0, 36, or 72 h and stained with Hoechst 33258 (*blue*, indicating total nuclei), Calcein-AM (*green*, indicating live cells), and PI (*red*, indicating dead cells). Images (LSM) were taken with a 40× objective, repeated three times with different cultures.

small interfering RNA, we cultured neurons from *casp2*$^{-/-}$ mice to assess possible context-dependent function of caspase-2. We treated cultures of wt and *casp2*$^{-/-}$ neurons with rotenone and measured the extent of apoptosis (Fig. 3*A*). No significant difference was observed in the basal level of cell death or apoptosis in *casp2*$^{-/-}$ neurons as compared with wt. Although rotenone treatment induced apoptosis in nearly 55% of the wt neurons after 36 h, in contrast, similarly treated *casp2*$^{-/-}$ neurons did not show a significant increase in apoptosis. To determine whether the *casp2*$^{-/-}$ neurons were dying via an alternative (nonapoptotic) mechanism, we also measured neuronal survival in *casp2*$^{-/-}$ neurons by Calcein-AM/PI staining (live/dead assay). Interestingly, after rotenone exposure, *casp2*$^{-/-}$ neurons showed a survival advantage ($p < 0.05$) as compared with wt (Fig. 3*B*). Even after 72 h of rotenone treatment, ~68% of wt neurons died compared with only about ~30% of the *casp2*$^{-/-}$ neurons. When we studied the mode of the delayed cell death in the *casp2*$^{-/-}$ neurons, the majority of the neuronal morphologies showed a preserved chromatin structure but with the loss of neurites and membrane damage (loss of Calcein-AM and PI staining without showing nuclear condensation or fragmentation), characteristics suggestive of necrosis (Fig. 3*C*). Taken together, these results indicate that after treatment with rotenone, caspase-2 is activated as the initiator caspase, and loss of caspase-2 is protective against rotenone-induced apoptosis as well as neuronal death.

*Loss of Caspase-2 Protects Neurons from Rotenone-induced Superoxide*—To determine whether rotenone-induced mitochondrial superoxide generation is responsible for caspase-2 activation and cytotoxicity, we conducted studies using a well known antioxidant, NAC, that is known to inhibit rotenone-induced superoxide (18, 19, 26). We found that rotenone induced superoxide generation, as determined by MitoSOX Red staining, in neuronal cultures within 1 h of treatment. No significant difference was observed in the extent of superoxide generation between wt and *casp2*$^{-/-}$ after rotenone treatment. Pretreatment with NAC significantly inhibited rotenone-induced superoxide generation (Fig. 4*A*) as well as cell death in the wt neurons (Fig. 4*B*), confirming a role for rotenone-induced superoxide generation in inducing neuronal cell death.

We further investigated the effect of NAC pretreatment on rotenone-induced caspase-2 cleavage (Fig. 4*C*). As determined by Western blotting, NAC treatment significantly inhibited the rotenone-induced caspase-2 cleavage. We then studied the effect of NAC treatment on rotenone-induced cell death in *casp2*$^{-/-}$ neuronal cultures (Fig. 4*C*). Interestingly, pretreatment with NAC did lead to significant inhibition of superoxide production in rotenone-treated *casp2*$^{-/-}$ neurons but did not provide any additional protection to *casp2*$^{-/-}$ neurons from rotenone-induced cell death (Fig. 4*D*). Collectively, the data suggest that caspase-2 is activated by rotenone-induced superoxide and plays a role in neuronal cell death.

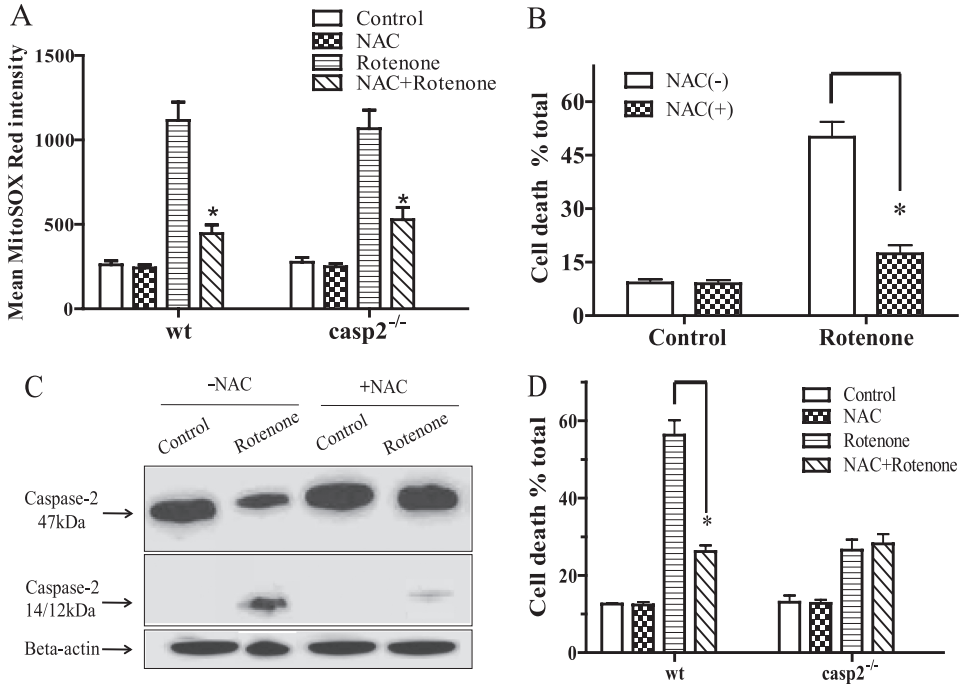


FIGURE 4. **Caspase-2 is activated by rotenone-induced mitochondrial superoxide.** Neurons were pretreated with or without 2 mM of NAC for 2 h and then exposed or not to the rotenone (0.3 $\mu$M) for 1 h for ROS measurement (*A*) and 36 h for cell death and caspase activation (*B–D*). *A*, after 1 h of rotenone treatment, superoxide generation was determined by staining cells with MitoSOX Red; LSM was used to acquire fluorescence images, and mean fluorescent intensity was determined by ImageJ (±S.E., $n = 150–200$ neurons/group); the experiment was repeated three times. *B*, cell viability was determined by Calcein-AM and PI staining (36 h treatment). *C*, caspase-2 activation was determined by Western blotting. *D*, cell viability in wt and *casp2*$^{-/-}$ neurons is shown. The *asterisk* (*) represents *p* values $<0.05$, comparing time-matched wt *versus* *casp2*$^{-/-}$ neurons.

We further investigated whether rotenone stimulates superoxide production and caspase-2 activation in another model and, if so, whether caspase-2 is required for cell death. For this we performed experiments on MEF from wt or *casp2*$^{-/-}$ mice (supplemental Fig. 2). Despite a similar extent of rotenone-induced superoxide production as determined by MitoSOX staining, *casp2*$^{-/-}$ MEFs showed significantly higher survival against rotenone treatment, suggesting that caspase-2 plays a role in superoxide-mediated cell death not only in neurons but also in other cell types.

*Caspase-2 Acts Upstream of Rotenone-induced Mitochondrial Apoptotic Events*—We further investigated how caspase-2 is involved in rotenone-induced apoptosis. Caspase-2 has been shown to induce mitochondrial outer membrane permeabilization (MOMP) that leads to the release of pro-apoptotic molecules from mitochondria (27–30). It is well documented that cytochrome *c* is released from the mitochondria after MOMP induction and, therefore, can be used as a reliable index of MOMP (31). To examine cytochrome *c* release in rotenone-treated wt and *casp2*$^{-/-}$ neurons, we performed immunofluorescence staining of the cells using a cytochrome *c* antibody (*green*), and as a control, the mitochondria were stained with MitoTracker Red (Fig. 5*A*). Cytochrome *c* staining exhibited a punctate pattern in the control neurons from wt and *casp2*$^{-/-}$ that overlapped with MitoTracker Red staining (Fig. 5*A*, *a* and *c*). Within 16 h of rotenone treatment, the wt neurons displayed a diffused cytochrome *c* staining pattern with a loss of mitochondrial localization indicative of its release from the mitochondria (Fig. 5*Ab*). In contrast, in the majority of rotenone-treated *casp2*$^{-/-}$ neurons, despite a fragmented pattern of the mitochondria, cytochrome *c* staining was still punctate and retained its mitochondrial localization (Fig. 5*Ad*). Quantitative analysis of the percentage of cells showing cytochrome *c* release confirmed that rotenone-induced cytochrome *c* release was significantly reduced in *casp2*$^{-/-}$ neurons compared with wt (Fig. 5*B*). In line with these data, we also found that loss of caspase-2 protected neurons from rotenone-induced loss of mitochondrial membrane permeability transition as determined by tetramethylrhodamine methyl ester staining (supplemental Fig. 3).

Next, we examined AIF nuclear translocation in rotenone-treated wt and *casp2*$^{-/-}$ neurons. AIF is another proapoptotic molecule that is released from the mitochondrial intermembranous space after MOMP. After its release, AIF translocates to the nucleus, where it induces large scale DNA fragmentation and chromatin condensation (32–34). To study AIF nuclear translocation, we performed immunofluorescence staining using AIF antibody (*red*); nuclei were stained with Hoechst 33258 (*blue*) (Fig. 5*C*). The quantification of the percentage of cells showing AIF nuclear translocation is shown in Fig. 5*D*. In the control wt or *casp2*$^{-/-}$ neurons, AIF retained its mitochondrial localization, as can be seen by its punctuate staining pattern (Fig. 5*C*, *a* and *e*). After 16 h of rotenone treatment, cells did not exhibit any significant release of AIF into the cytosol or the nucleus in either wt or *casp2*$^{-/-}$ neurons (Fig. 5*C*, *b* and *f*). After 24 h of rotenone treatment, there was a significant increase in the percentage of wt neurons (~22%) in which AIF showed loss of punctate staining pattern with a concomitant increase in nuclear and cytoplasmic localization. This pattern in wt increased further after 36 h when more than 51% neurons

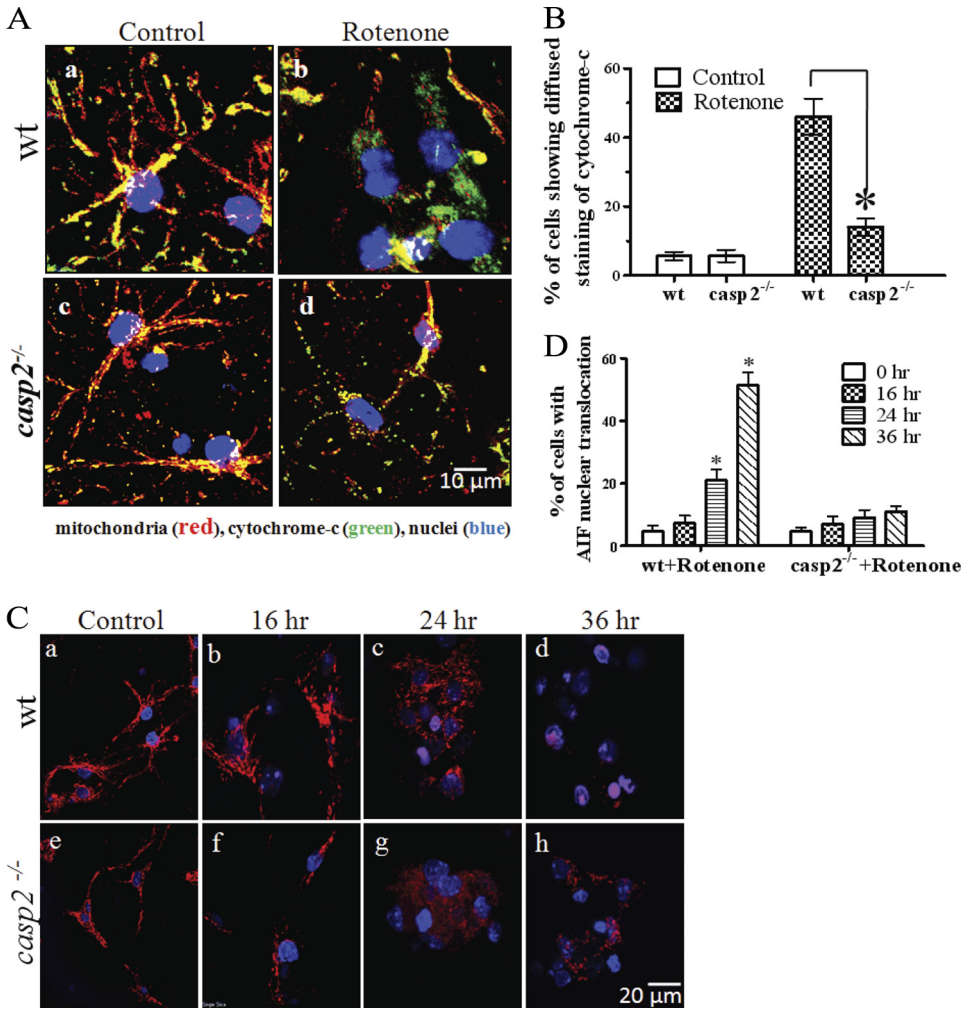


FIGURE 5. **Loss of caspase-2 prevents rotenone-induced release of cytochrome *c* and AIF from mitochondria.** Cortical neurons cultured from wt and *casp2*$^{-/-}$ were treated with rotenone (0.3 μM) for 16 h. *A*, neurons were co-stained with MitoTracker Red for mitochondria, cytochrome *c* (*green*), and Hoechst 33258 for nuclei (*blue*), and overlay images are shown. Mitochondrial localization of cytochrome *c* can be seen as yellow fluorescence due to colocalization of green fluorescence with *red* (mitochondria). Cytochrome *c* release can be identified as an increase in *green* fluorescence with a diffused pattern and a decrease in the *yellow* fluorescence localized to mitochondria. Images were obtained with a 60× objective, shown as 3 times the digital magnification. *B*, a histogram shows the % of cells showing cytochrome *c* translocation to cytosol. Loss of caspase-2 prevents rotenone-induced nuclear translocation of AIF. *C*, cortical neurons cultured from wt and *casp2*$^{-/-}$ were treated with rotenone (0.3 μM) for 16, 24, and 36 h and were stained for AIF (*red*) and nuclei-stained with Hoechst 33258 (*blue*). The overlay images of AIF and nuclear staining are shown at 60× magnification (2× digital zoom). The AIF translocation to the nuclei can be identified by the appearance of a *magenta* color due to co-localization with blue fluorescence (nuclei) with red (AIF). *D*, a histogram shows the % of cells showing AIF nuclear translocation. At least 150–200 neurons were counted per group. Data (±S.E.) were derived from three separate experiments. The *asterisk* (*) represents *p* values <0.05, comparing time-matched wt *versus* *casp2*$^{-/-}$ neurons.

showed AIF nuclear translocation (Fig. 5*Cd*). In contrast, even after 36 h of rotenone treatment only a few nuclei in the *casp2*$^{-/-}$ neurons showed nuclear localization of AIF (~11%). This response was significantly lower than that observed in wt (Fig. 5*C*, *d* and *h*), suggesting an involvement of caspase-2 upstream to AIF release in rotenone-induced neuronal apoptosis. Thus, the results indicate a role of caspase-2 in the induction of MOMP during rotenone-induced toxicity in neurons.

One way by which caspase-2 can induce MOMP is by activating Bid and Bax (28, 35). We examined whether rotenone treatment leads to Bid cleavage and, if so, whether this response is affected by loss of caspase-2. In wt neurons, rotenone treatment induced the truncation of Bid with a decrease in the 21-kDa form and a subsequent increase in the 15-kDa form, as determined by Western blotting (Fig. 6*A*). However, compared with wt, the truncation of Bid was significantly reduced in rotenone-treated *casp2*$^{-/-}$ neurons, suggesting an involvement of caspase-2 in rotenone-induced Bid truncation.

We next examined rotenone-induced Bax activation in wt and *casp2*$^{-/-}$ neurons by immunolabeling the cells using the Bax 6A7 antibody that recognizes the active Bax (Fig. 6*B*). In both wt and *casp2*$^{-/-}$ controls, no significant Bax 6A7 fluorescence staining was detected, indicating that in untreated neurons Bax was not present in the active form (Fig. 6*B*, *a* and *c*). After rotenone treatment, there was a significant increase in the number of wt neurons exhibiting Bax 6A7 staining compared with the controls (Fig. 6*Bb*), suggesting Bax activation. In contrast, very few rotenone-treated *casp2*$^{-/-}$ neurons exhibited Bax 6A7 staining (Fig. 6*Bd*). Quantitative analysis of Bax-stained cells showed that rotenone-induced Bax activation was significantly less in *casp2*$^{-/-}$ neurons compared with that in wt (Fig. 6*C*).

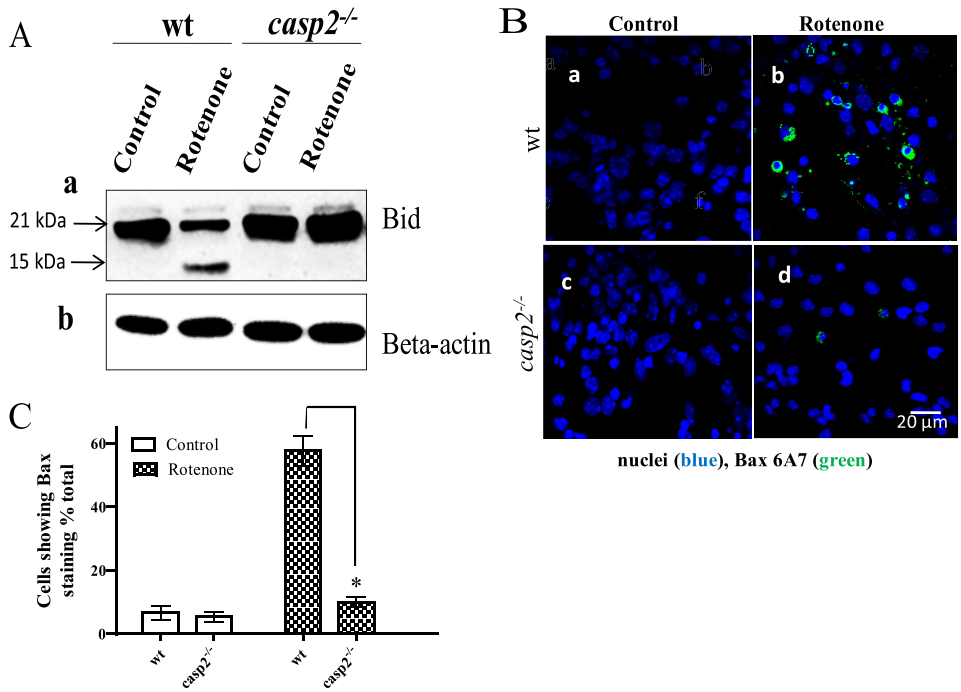


FIGURE 6. **Loss of caspase-2 prevents rotenone-induced Bid cleavage and Bax activation.** Cortical neurons cultured from wt and *casp2*$^{-/-}$ were treated with rotenone (0.3 $\mu$M) for the indicated times. *A*, a representative Western blot performed using WCL shows Bid cleavage in rotenone-treated wt neurons (36 h treatment) that was prevented in the absence of caspase-2. Full-length Bid appears at 21 kDa, and cleaved Bid is at 15 kDa. $\beta$-Actin was used as a loading control for respective blots. *B*, immunocytochemistry for Bax translocation using Bax 6A7 (*green*) antibody that recognizes active Bax is shown. Overlay images of Bax staining and nuclei (Hoechst 33258 in *blue*) are shown (60×). Bax staining was observed only when active Bax was present. *C*, a histogram show the % of cells showing Bax activation (±S.E., $n$ = 150–200 neurons/group); the experiment was repeated three times. The *asterisk* (*) represents $p$ values <0.05, comparing time matched wt *versus* *casp2*$^{-/-}$ neurons.

*Caspase-2 Activation Is Upstream of Caspase-9 and Caspase-3 Activation*—Release of cytochrome *c* from mitochondria results in formation of the apoptosome with a subsequent activation of caspase-9 and caspase-3. Because our earlier results indicated that caspase-2 is an initiator caspase during rotenone-induced apoptosis, we next examined rotenone-induced activation of caspase-9 and caspase-3 in wt and *casp2*$^{-/-}$ neurons. To detect only active caspases, after 36 h of rotenone treatment, the WCL were incubated with b-VAD-fmk. The caspases trapped by the inhibitor were isolated using streptavidin, probed with caspase-3 and caspase-9 antibodies, and then analyzed by Western blotting. The WCL without streptavidin pulldown are also shown for comparison (Fig. 7*B*). After treatment with rotenone for 36 h, there was a significant increase in the activation of caspase-3 and -9 in the wt neurons (Fig. 7*A*). By contrast, in the *casp2*$^{-/-}$ neurons, the levels of active caspase-3 and -9 were detected only at very low levels. We could not detect the activation of caspase-8 either in wt or *casp2*$^{-/-}$ neurons after rotenone treatment (data not shown). We also performed immunofluorescence microscopy using an antibody that detects cleaved caspase-3 (active subunit) followed by its quantification (Fig. 7, *C* and *D*). In untreated wt neurons, very few cells showed active caspase-3 (~6% in wt and ~7% in *casp2*$^{-/-}$). After treatment with rotenone for 36 h, ~47% of the wt neurons stained positive for the cleaved caspase-3 (Fig. 7*Cb*). By contrast, no significant increase in active caspase 3 was observed in the rotenone-treated *casp2*$^{-/-}$ neurons (Fig. 7*Cd*).

The use of a commercial caspase inhibitor showed that inhibition of caspase-2 provided maximum protection from rotenone-induced neuronal death. On the other hand, treatment with caspase-9 or caspase-3 inhibitors produced less protection of the neurons from rotenone toxicity. Similarly, the caspase-8 inhibitor did not provide any significant protection from neuronal cell death (supplemental Fig. 4). Collectively, these results suggest a selective initiator role for caspase-2 in rotenone-induced neuronal apoptosis.

*Autophagy Is Induced in casp2*$^{-/-}$ *Neurons and Delays Rotenone-induced Cell Death*—Loss of caspase-2 inhibited rotenone-induced apoptosis and delayed cell death in the cortical neurons. Therefore, it was important to determine whether *casp2*$^{-/-}$ neurons survive better in the presence of rotenone-induced oxidative damage or if the remaining *casp2*$^{-/-}$ neurons show a delayed cell death by an alternative pathway in the absence of apoptosis. We and others have shown that, besides inducing apoptosis, oxidative stress can also induce autophagy (26, 36–40). Thus, we examined whether rotenone induces autophagy in *casp2*$^{-/-}$ neurons. Autophagy can be detected by examining the conversion of cytosolic LC3-I to lipidated, autophagosome membrane-bound LC3-II. These autophagosomes in turn form autophagolysosomes by fusing with lysosomes (41). Immunocytochemistry using LC3 antibody was performed to study its redistribution after rotenone treatment. In addition, LysoTracker Red colabeling was performed to visualize fusion between lysosomes and autophagosomes (Fig. 8*A*). In the control wt and *casp2*$^{-/-}$ neurons, LC3 was distributed predominantly as diffuse green fluorescence in the cytoplasm and nucleus with very little lysosomal staining. After rotenone treatment, wt neurons retained a diffused staining pattern of

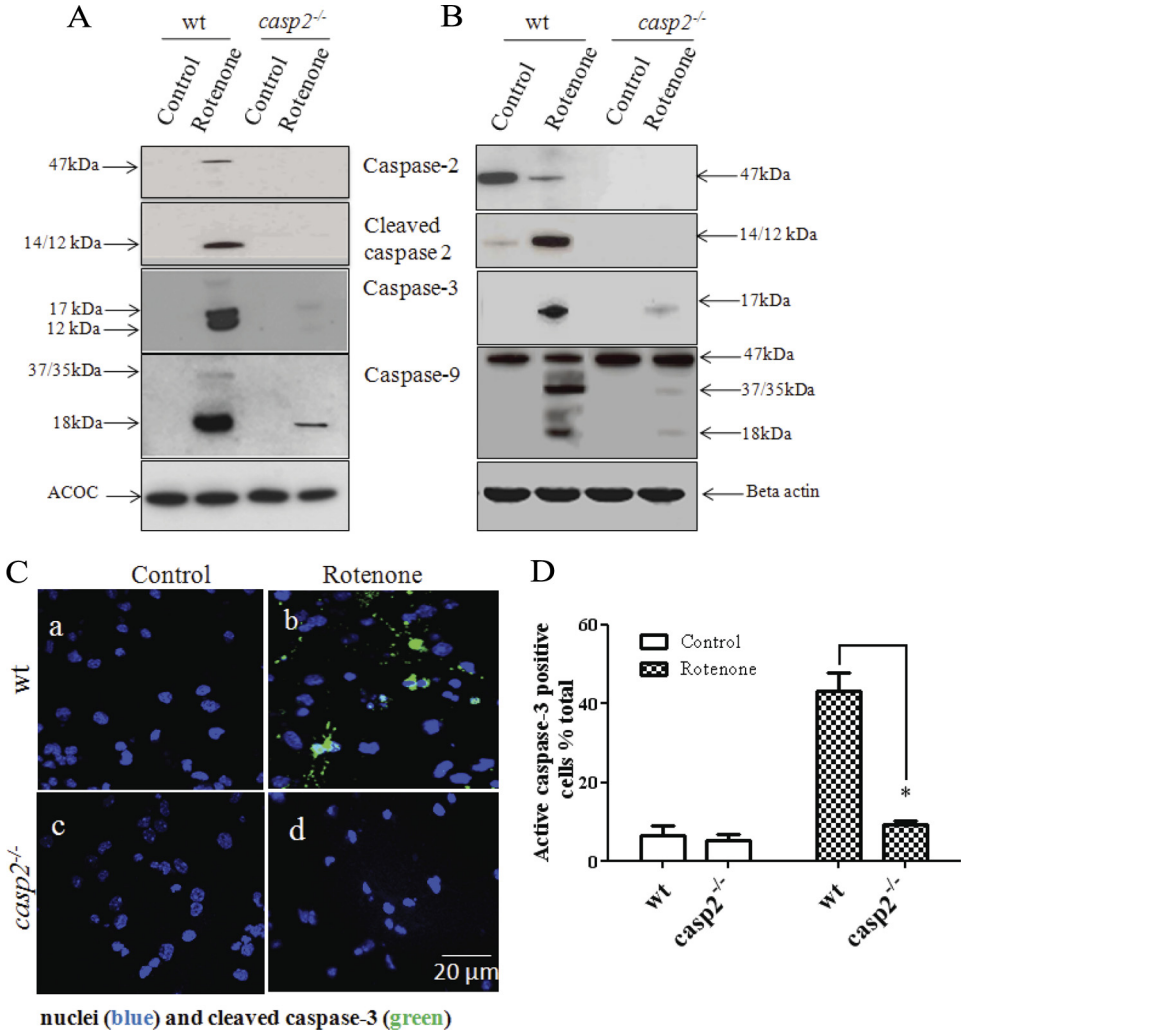


FIGURE 7. **Effect of rotenone on caspase-9 and caspase-3 activation in wt and *casp2*$^{-/-}$ neurons.** Neurons from wt and *casp2*$^{-/-}$ cultures were either untreated or exposed to rotenone. *A* and *B*, neurons were incubated with rotenone for ~36 h, and b-VAD-fmk(50 $\mu$M) was added 2 h before harvesting. Cell lysates were subjected to streptavidin pulldown (*A*) and/or preparation of WCL (*B*) followed by assessment for caspase-2, -3, and -9 by immunoblotting. Western blot analysis was performed by standard procedures. The same blots were subsequently probed with acetyl-CoA carboxylase (*ACOC*) or $\beta$-actin and used as a control for precipitation and loading. Shown are representative blots; the experiment was repeated three times. *C*, shown is immunofluorescence staining for active caspase-3 (*green*) and nuclei counterstained with Hoechst 33258 (*blue*). Shown are the representative overlay images at 60× magnifications. *D*, a histogram shows the % of cells with active caspase-3 staining, quantified by counting the numbers of cells with active caspase-3 and the total number of cells (±S.E., $n$ = 150–200 neurons/group); the experiment was repeated three times. The *asterisk* (*) represents $p$ values <0.05, comparing time matched wt *versus* *casp2*$^{-/-}$ neurons.

LC3 with very little (non significant) increase in lysosomal staining (Fig. 8*A*). By contrast, rotenone-treated *casp2*$^{-/-}$ neurons at 16 h showed a characteristic punctate pattern of LC3 immunofluorescence that was dispersed through the cell. Furthermore, a fraction of the *casp2*$^{-/-}$ neurons demonstrated a colocalization of LC3 with lysosomes, suggesting the formation of autophagosome and autophagolysosomes. After 36 h of rotenone treatment of *casp2*$^{-/-}$ neurons, the punctate feature representing the autophagosomes gradually faded/vanished, presumably due to the fusion of autophagosome with lysosome resulting in degradation of LC3 and an associated loss of staining.

We also performed Western blotting for LC3. Because LC3-II is continually degraded within autophagolysosomes during autophagy, we treated the neurons in the presence of pepstatin A (1 $\mu$M) and E-64d (10 $\mu$M), which are lysosomal inhibitor, and the samples were prepared for Western blotting for LC3 to demonstrate autophagic flux (42). A significant increase in LC3-II was detected in rotenone-treated *casp2*$^{-/-}$ neurons but not in wt neurons, further corroborating the evidence of enhanced autophagy in the rotenone-treated *casp2*$^{-/-}$ neurons (Fig. 8, *B* and *C*). We also performed Western blotting for Beclin1, a component of the phosphatidylinositol 3-kinase complex known to increase during autophagy (43). A significant and consistent increase was observed in the levels of Beclin1 in rotenone-treated *casp2*$^{-/-}$ neurons as compared with wt neurons after rotenone treatment. It is important to note that in rotenone-treated wt neurons, Beclin1 levels decreased significantly (Fig. 8, *D* and *E*). It has been shown that Beclin1 is cleaved by caspases during apoptosis (44), which is consistent with our data that indicate an induction of apoptosis in wt neurons after treatment with rotenone.

Next, we examined the role of autophagy on cell death or cell survival. Because transfecting the young adult neurons in cul-

ture was associated with potential technical difficulties, we were restricted to the use of pharmacological inhibitors of autophagy. The inhibition of autophagy at an early stage by 3-methyladenine and at a late stage by bafilomycin A1 completely abolished the protective effect of loss of caspase-2 during rotenone-induced cell death (Fig. 8*F*). The enhanced death

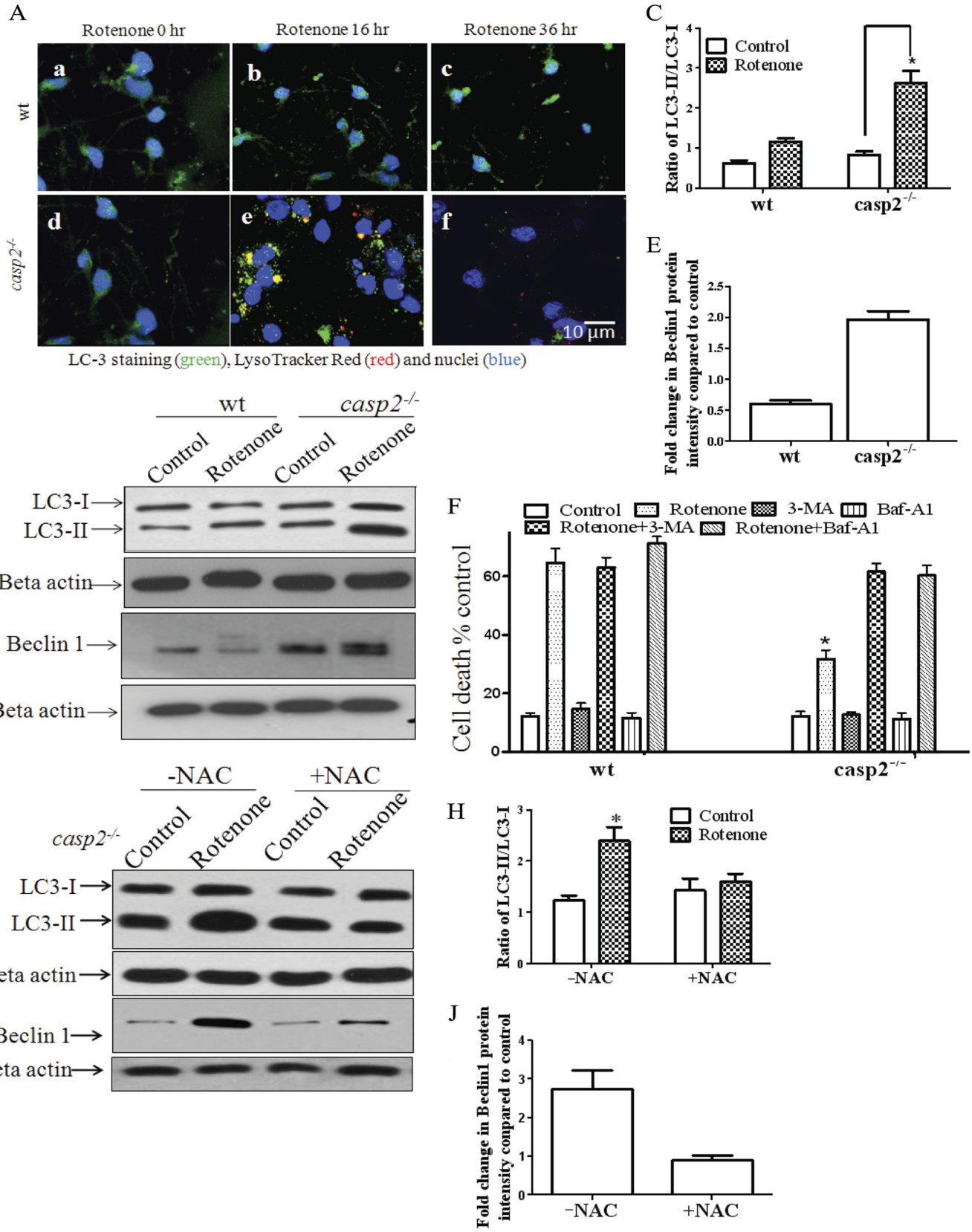

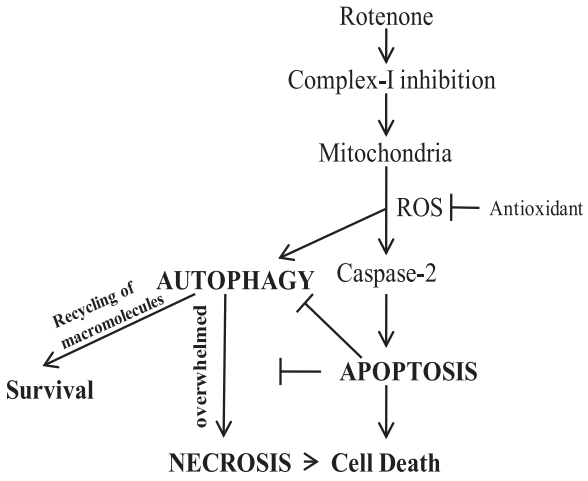


FIGURE 9. **Schematic illustration of the proposed pathways for rotenone-induced cell death in neurons; rotenone acts on mitochondria by inhibiting complex I, thereby enhancing the ROS production.** Caspase-2 is activated as an initiator caspase by ROS to induce apoptosis upstream to mitochondria. Caspase-2 inhibition rescues apoptotic response toward rotenone treatment. In this case oxidative stress triggers an autophagic response that is normally suppressed in the presence of apoptosis. In the absence of apoptosis, autophagy promotes survival, but ultimately the cells show a delayed necrotic cell death.

in the absence of caspase-2 was necrotic in nature as determined by an increase in PI uptake with loss of Calcein-AM and without features of apoptosis, such as chromatin condensation and nuclear fragmentation. Thus, loss of caspase-2 results in enhanced autophagy after rotenone treatment and thereby delays neuronal death.

Finally, to find whether rotenone-mediated oxidative stress causes enhanced autophagy in *casp2*$^{-/-}$ neurons, we accessed autophagy in the presence of NAC (an antioxidant) in rotenone-treated *casp2*$^{-/-}$ neurons. Autophagy was determined by Western blotting to measure the LC3-II/LC3-I ratio and Beclin1 levels. As shown in Fig. 8, *G–J*, we found that NAC pretreatment inhibited rotenone-induced increase in LC3-II/LC3-I ratio as well as Beclin1 levels in *casp2*$^{-/-}$ neurons, indicating that NAC inhibits rotenone-induced autophagy. These results suggest that autophagy was induced in response to oxidative stress induced by rotenone when the neurons cannot undergo apoptosis due to lack of caspase-2 (Fig. 9).

## DISCUSSION

The function of caspase-2 has remained enigmatic, partly due to the fact that mice lacking caspase-2 are viable and fertile with only minor apoptotic defects in certain cell types (22). However, several studies have implicated caspase-2 as a crucial mediator of apoptosis in a context-dependent manner, which includes heat shock (25), DNA damage (29), and cytoskeleton disruption (45). Previous studies from our laboratory demonstrated that *casp2*$^{-/-}$ mice display premature aging-related traits and significantly higher levels of oxidized proteins in liver than wt mice, indicating an inability to remove the oxidatively damaged cells (46). Furthermore, caspase-2 functions in oxidative stress-induced apoptosis are coming to light (47, 48). In this regard a present report provides strong evidence for the role of caspase-2 in mitochondrial-mediated oxidative stress-induced apoptosis in neurons. Moreover, involvement of caspase-2 in rotenone-induced cell death is not restrictive to neuronal cell type but also non-neuronal cell type (MEFs).

The present study was performed employing cultures of young adult cortical neurons to identify the initiator caspase and its role in neuronal apoptosis induced by mitochondrial oxidative stress inducing agent, rotenone. Our results demonstrate 1) a role of caspase-2 as an initiator caspase during mitochondrial oxidative stress-induced apoptosis, 2) that caspase-2 acts upstream of mitochondria during rotenone-induced apoptosis, 3) that loss of caspase-2 protect neurons from apoptosis as well as cell death, and 4) that rotenone induces autophagy in *casp2*$^{-/-}$ neurons that delays the cell death and neurons eventually die via necrotic cell death.

Caspase-2 is one of the most conserved caspases and has been recognized as both an initiator and an effector caspase depending upon the cell type and type of stressor (49–55). In the case of neurons, the initiator role of caspase-2 has remained controversial. Previous studies have defined a role of caspase-2 as an initiator caspase in neuronal apoptosis during serum deprivation (56), β-amyloid-mediated toxicity (57), and oxidative stress-induced apoptosis of neuronal stem cells (47), where it plays an important role in apoptosis induction. On the other hand, other studies have suggested that caspase-2 may be activated in response to different stimuli in neurons and other cell types but may not be essential for induction of apoptosis (22,54). In our experiments employing *in situ* trapping of initiator caspases approach, which is a valuable method to identify initiator caspases (6, 25), we identified caspase-2 as the initiator caspase during rotenone-induced apoptosis in neurons. Furthermore, using neurons that lack caspase-2, our data clearly indicate that caspase-2 plays an important role in mediating neuronal apoptosis during mitochondrial oxidative stress. The initiator role of caspase-2 was further supported by the observations that loss of caspase-2 inhibited rotenone-induced caspase-3 and caspase-9 activation and a caspase-2 inhibitor

FIGURE 8. **Loss of caspase-2 promotes autophagy after rotenone treatment.** Neurons from wt and *casp2*$^{-/-}$ mice were treated with rotenone (0.3 μM). *A*, shown is immunofluorescence for LC3 (*green*). Cells were counterstained with LysoTracker Red (*red*) and nuclei with Hoechst 33258 (*blue*). An increase in punctate pattern of LC3 (*green*), LysoTracker Red, and their colocalization (*yellow*) indicate an increase in autophagy. Shown are the representative overlay images at 60× magnifications with 2× digital zoom. *B* and *C*, LC3-I (18 kDa) and LC3-II (16 kDa) induction and conversion and LC3-II/LC3-I ratios were determined by Western blot using an antibody specific to LC3; β-actin was used as loading control. Cells were treated with rotenone in the presence of pepstatin A (1 μM) and E-64d (10 μM), and WCL were prepared at the indicated times (*, for $p < 0.001$, $n = 3$). All values are shown as the mean ± S.E. *D*, Western blotting for Beclin1 was performed using WCL, and β-actin served as the loading control. *E*, -fold change in Beclin1 intensity was determined using ImageJ densitometry analysis software, and values are shown as the mean ± S.E. ($n = 3$). *F*, cell viability analysis of rotenone-treated wt and *casp2*$^{-/-}$ neurons in the presence of autophagy inhibitors 3-methyladenine (*3-MA*; 1 mM) and bafilomycin A1 (*Baf-A1*; 10 nM) is shown. Data (±S.E.) were derived from three separate experiments. The *asterisk* (*) represents *p* values <0.05 comparing rotenone-treated wt *versus casp2*$^{-/-}$ neurons. *G* and *I*, representative Western blots for LC3 (*G*) or Beclin1 (*I*) in the presence or absence of NAC in rotenone-treated *casp2*$^{-/-}$ neurons are shown. For LC3 and Beclin1, samples were prepared as described above. *H* and *J*, -fold change in LC3-II/LC3-I ratio or Beclin1 intensity compared with β-actin (loading control) was determined using ImageJ densitometry analysis software, and values are shown as the mean ± S.E. ($n = 3$).

provided maximum protection from cell death compared with other caspase inhibitors used in the study.

In the present study we found that rotenone-induced apoptosis in the cultures of young adult cortical neurons was mainly due to its capacity to generate mitochondrial superoxide, which is in agreement with previous observations (18, 19, 26). Interestingly, we also found that caspase-2 activation was rotenone-induced superoxide-dependent. We suggested that if caspase-2 is involved in mitochondrial oxidative stress-induced cell death, then inhibition of superoxide should not provide further protection from cell death in *casp2*$^{-/-}$ neurons. In line with this hypothesis, pretreatment of *casp2*$^{-/-}$ neurons with antioxidant did not provide further protection to *casp2*$^{-/-}$ neurons from rotenone-induced cell death. Thus, our data suggest that caspase-2 is activated by rotenone-induced superoxide and plays a role in apoptotic cell death. However, in the present study we did not determine, 1) how superoxide activates caspase-2 and 2) if there is a particular species of superoxide or ROS that is responsible for caspase-2 activation and needs further investigation. Based on the literature, the structure of caspase-2 carries the maximum number of cysteines among the caspase family that includes a cysteine at the processing site and also a central disulfide bridge that leads to dimer stabilization in caspase-2 (58). Cysteine is an oxidative target because of the reactivity of the thiol group that is susceptible to modification by free radicals that may modulate the activity of these proteins, thus making caspase-2 a target for oxidation-based regulation. Furthermore, Madesh *et al.* (48) showed that incubation with superoxide induced caspase-2 cleavage and, hence, suggested that $O_2^-$ triggers caspase-2 cleavage through an as yet unidentified mechanism. They also showed that hydrogen peroxide did not recapitulate the effects of superoxide in promoting caspase-2 activation. Moreover, in agreement with these observations, we found that loss of caspase-2 protected against rotenone-induced neuronal cell death but not hydrogen peroxide-induced cell death (data not shown). Together these results indicate that caspase-2 may be more specifically involved in superoxide but not peroxide-mediated cell death and needs further investigation.

Previous studies performed to understand the mechanism of rotenone-induced apoptosis in various models showed an involvement of the intrinsic pathway of apoptosis that leads to activation of caspase-3 and caspase-9 after cytochrome *c* release (16–20). In agreement with previous observations, our results also demonstrate that neuronal cultures from young adult mice engage the intrinsic pathway of apoptosis. In addition, the present study demonstrates caspase-2 activation as an upstream event that engages the mitochondrial-dependent apoptotic pathway by inducing the release of cytochrome *c* and AIF from the mitochondria. One way by which caspase-2 has been shown to modulate mitochondrial release of apoptogenic proteins is by modulating the proapoptotic members of Bcl-2 protein family namely, Bid and Bax (28, 35). In the present study we did find inhibition of rotenone-induced Bid and Bax activation in cells lacking caspase-2, further suggesting that caspase-2 induces MOMP in neurons after rotenone treatment. However, previously it has been shown that superoxide-induced MOMP requires Bak for cytochrome *c* release in a Bax-independent manner. Using the similar system (*bax*$^{-/-}$, *bak*$^{-/-}$, and *bax*$^{-/-}$ *bak*$^{-/-}$ MEFs), indeed we found that despite the difference in the system used to generate superoxide, cytochrome *c* release was dependent on Bak but not Bax (supplemental Fig. 5).

It has been reported that elimination of certain caspases can be compensated by the activation of other caspases (25, 59, 60). For example, Troy *et al.* (61) found that caspase-2 plays a predominant role during nerve growth factor deprivation-induced cell death; however, in the absence of caspase-2, a compensatory switch to the caspase-9 pathway is observed (54). In the present study, we found that in the *casp2*$^{-/-}$ neurons the basal level of caspase-9 was higher than the wt (data not shown), which is consistent with the report by Troy *et al.* (54). However, we did not observe a compensatory activation of caspase-9 or caspase-8 in response to rotenone treatment in *casp2*$^{-/-}$ neurons. Moreover, these neurons die a delayed necrotic cell death that further suggested a role of caspase-independent apoptosis. Thus, compensatory caspase activation may depend upon the type of stimulus and the cell type.

Although *casp2*$^{-/-}$ neurons did not show compensatory caspase activation after rotenone treatment in the present case, they did show induction of autophagy in response to rotenone-mediated oxidative stress. Autophagy, which is a tightly regulated process, leads to degradation of intracellular components via the lysosome (62). It has been shown to be both a cell survival and a cell death pathway (63). Our results define a survival role for autophagy, as inhibition of autophagy abolished the survival advantage of rotenone-treated *casp2*$^{-/-}$ neurons. On the other hand, we also found that these neurons eventually die a delayed cell death with features of necrosis. It seems that rotenone-treated *casp2*$^{-/-}$ neurons that cannot undergo apoptotic cell death induce autophagy as an alternate mechanism to combat oxidative stress induced by rotenone for the removal of the damaged organelles and macromolecules. However, eventually the autophagic process is overwhelmed by the massive amount of damaged material it is trying to clear. This can lead to cell death through a non-apoptotic mechanism, accounting for a delayed necrotic cell death. Therefore, our data support the hypothesis that autophagy can be both a cell survival mechanism and a cell death pathway depending on the extent of cellular damage and the efficiency of the autophagic process (64). It is important to note that in the present study we did not employ general caspase inhibitors that may produce nonspecific affects that include autophagy activation (65). Our data are based on the inhibition of apoptosis through inhibition of caspase-2 that is involved in the initiation pathway of apoptosis. Our data are in accordance with a previous study in which it was found that the MEFs from double-knock-out *bax*$^{-/-}$ *bak*$^{-/-}$ mice fail to undergo apoptosis when treated with death stimulus but instead manifest a massive autophagy followed by delayed cell death (64). Bax and Bak are two multidomain protein members of the Bcl2 family that are required for MOMP, which is one of the decisive steps in apoptotic cell death (66). However, autophagy was not induced when apoptosis was inhibited by other perturbations, such as in *apaf1*$^{-/-}$ and *caspase-9*$^{-/-}$ mouse embryonic fibroblasts or the addition of the caspase inhibitor benzyloxycarbonyl-VAD-fmk to wt mouse embryonic fibroblasts. Thus, along with these observa-

tions, our present data support the hypothesis that inhibition of apoptosis upstream to MOMP may be a decisive factor for the cells to undergo autophagy.

Taken together the present study identifies a role of caspase-2 as an initiator caspase in mitochondrial oxidative stress-induced apoptosis in the cultures of young adult cortical neurons. When apoptosis is inhibited at an early stage, the neuron undergoes autophagy that delays cell death (Fig. 9). In cells such as neurons, who have very limited capacity to regenerate, the prevention of any kind of damage or loss is of utmost importance. Thus, understanding the mechanism of cell death and the alternate pathways becomes important in defining the pharmaceutical approaches to prevent neuronal damage.

*Acknowledgments—We thank Dr. Junying Yuan of Harvard University and Dr. Carol Troy of Columbia University for providing the casp2$^{-/-}$ mice and Dr. Muniswamy Madesh of Temple University for providing bax$^{-/-}$, bak$^{-/-}$,* and *bax$^{-/-}$ bak$^{-/-}$ DKO MEFs. We thank Dr. Victoria Centonze-Frohlich for contributions and guidance on the microscopy experiments. Images were generated in the Core Optical Imaging Facility, which is supported by University of Texas Health Science Center-San Antonio and National Institutes of Health Grants P30 CA54174 (NCI; to the San Antonio Cancer Institute), P30 AG013319 (NIA; to the Nathan Shock Center), and P01 AG19316 (NIA). We also thank Dr. Christie Jones and Sonya Karbach for help in preparation of the manuscript and Michelle Bendele for assistance in mouse breeding.*

## REFERENCES


1. Keating, D. J. (2008) *J. Neurochem.* **104,** 298–305
2. Trushina, E., and McMurray, C. T. (2007) *Neuroscience* **145,** 1233–1248
3. Lin, M. T., and Beal, M. F. (2006) *Nature* **443,** 787–795
4. Bredesen, D. E., Rao, R. V., and Mehlen, P. (2006) *Nature* **443,** 796–802
5. Baliga, B. C., Read, S. H., and Kumar, S. (2004) *Cell Death Differ.* **11,** 1234–1241
6. Boatright, K. M., Renatus, M., Scott, F. L., Sperandio, S., Shin, H., Pedersen, I. M., Ricci, J. E., Edris, W. A., Sutherlin, D. P., Green, D. R., and Salvesen, G. S. (2003) *Mol. Cell* **11,** 529–541
7. Renatus, M., Stennicke, H. R., Scott, F. L., Liddington, R. C., and Salvesen, G. S. (2001) *Proc. Natl. Acad. Sci. U.S.A.* **98,** 14250–14255
8. Budihardjo, I., Oliver, H., Lutter, M., Luo, X., and Wang, X. (1999) *Annu. Rev. Cell Dev. Biol.* **15,** 269–290
9. Robertson, G. S., Crocker, S. J., Nicholson, D. W., and Schulz, J. B. (2000) *Brain Pathol.* **10,** 283–292
10. Friedlander, R. M. (2003) *N. Engl. J. Med.* **348,** 1365–1375
11. Lee, J. A. (2009) *BMB Rep.* **42,** 324–330
12. Shaw, C. A., and Höglinger, G. U. (2008) *Neuromolecular Med.* **10,** 1–9
13. Sharma, L. K., Lu, J., and Bai, Y. (2009) *Curr. Med. Chem.* **16,** 1266–1277
14. Takayanagi, R., Takeshige, K., and Minakami, S. (1980) *Biochem. J.* **192,** 853–860
15. Turrens, J. F., and Boveris, A. (1980) *Biochem. J.* **191,** 421–427
16. Pei, W., Liou, A. K., and Chen, J. (2003) *FASEB J.* **17,** 520–522
17. Lee, J., Huang, M. S., Yang, I. C., Lai, T. C., Wang, J. L., Pang, V. F., Hsiao, M., and Kuo, M. Y. (2008) *Biochem. Biophys. Res. Commun.* **371,** 33–38
18. Khar, A., Ali, A. M., Begum, Z., Pardhasaradhi, B. V., and Varalakshmi, C. (1999) *Indian J. Biochem. Biophys.* **36,** 77–81
19. Li, N., Ragheb, K., Lawler, G., Sturgis, J., Rajwa, B., Melendez, J. A., and Robinson, J. P. (2003) *J. Biol. Chem.* **278,** 8516–8525
20. Isenberg, J. S., and Klaunig, J. E. (2000) *Toxicol. Sci.* **53,** 340–351
21. Lesuisse, C., and Martin, L. J. (2002) *J. Cereb. Blood Flow Metab.* **22,** 935–950
22. Bergeron, L., Perez, G. I., Macdonald, G., Shi, L., Sun, Y., Jurisicova, A., Varmuza, S., Latham, K. E., Flaws, J. A., Salter, J. C., Hara, H., Moskowitz, M. A., Li, E., Greenberg, A., Tilly, J. L., and Yuan, J. (1998) *Genes Dev.* **12,** 1304–1314
23. Brewer, G. J., and Torricelli, J. R. (2007) *Nat. Protoc.* **2,** 1490–1498
24. Boatright, K. M., and Salvesen, G. S. (2003) *Curr. Opin. Cell Biol.* **15,** 725–731
25. Tu, S., McStay, G. P., Boucher, L. M., Mak, T., Beere, H. M., and Green, D. R. (2006) *Nat. Cell Biol.* **8,** 72–77
26. Chen, Y., Azad, M. B., and Gibson, S. B. (2009) *Cell Death Differ.* **16,** 1040–1052
27. Lassus, P., Opitz-Araya, X., and Lazebnik, Y. (2002) *Science* **297,** 1352–1354
28. Guo, Y., Srinivasula, S. M., Druilhe, A., Fernandes-Alnemri, T., and Alnemri, E. S. (2002) *J. Biol. Chem.* **277,** 13430–13437
29. Zhivotovsky, B., and Orrenius, S. (2005) *Biochem. Biophys. Res. Commun.* **331,** 859–867
30. Robertson, J. D., Enoksson, M., Suomela, M., Zhivotovsky, B., and Orrenius, S. (2002) *J. Biol. Chem.* **277,** 29803–29809
31. Kluck, R. M., Bossy-Wetzel, E., Green, D. R., and Newmeyer, D. D. (1997) *Science* **275,** 1132–1136
32. Susin, S. A., Lorenzo, H. K., Zamzami, N., Marzo, I., Snow, B. E., Brothers, G. M., Mangion, J., Jacotot, E., Costantini, P., Loeffler, M., Larochette, N., Goodlett, D. R., Aebersold, R., Siderovski, D. P., Penninger, J. M., and Kroemer, G. (1999) *Nature* **397,** 441–446
33. Daugas, E., Susin, S. A., Zamzami, N., Ferri, K. F., Irinopoulou, T., Larochette, N., Prévost, M. C., Leber, B., Andrews, D., Penninger, J., and Kroemer, G. (2000) *FASEB J.* **14,** 729–739
34. Cregan, S. P., Fortin, A., MacLaurin, J. G., Callaghan, S. M., Cecconi, F., Yu, S. W., Dawson, T. M., Dawson, V. L., Park, D. S., Kroemer, G., and Slack, R. S. (2002) *J. Cell Biol.* **158,** 507–517
35. Bonzon, C., Bouchier-Hayes, L., Pagliari, L. J., Green, D. R., and Newmeyer, D. D. (2006) *Mol. Biol. Cell* **17,** 2150–2157
36. Lemasters, J. J., Nieminen, A. L., Qian, T., Trost, L. C., Elmore, S. P., Nishimura, Y., Crowe, R. A., Cascio, W. E., Bradham, C. A., Brenner, D. A., and Herman, B. (1998) *Biochim. Biophys. Acta* **1366,** 177–196
37. Tiwari, M., Bajpai, V. K., Sahasrabuddhe, A. A., Kumar, A., Sinha, R. A., Behari, S., and Godbole, M. M. (2008) *Carcinogenesis* **29,** 600–609
38. Kiffin, R., Bandyopadhyay, U., and Cuervo, A. M. (2006) *Antioxid. Redox Signal.* **8,** 152–162
39. Kunchithapautham, K., and Rohrer, B. (2007) *Autophagy* **3,** 433–441
40. Chen, Y., McMillan-Ward, E., Kong, J., Israels, S. J., and Gibson, S. B. (2007) *J. Cell Sci.* **120,** 4155–4166
41. Kabeya, Y., Mizushima, N., Ueno, T., Yamamoto, A., Kirisako, T., Noda, T., Kominami, E., Ohsumi, Y., and Yoshimori, T. (2000) *EMBO J.* **19,** 5720–5728
42. Mizushima, N., and Yoshimori, T. (2007) *Autophagy* **3,** 542–545
43. Kihara, A., Kabeya, Y., Ohsumi, Y., and Yoshimori, T. (2001) *EMBO Rep.* **2,** 330–335
44. Luo, S., and Rubinsztein, D. C. (2010) *Cell Death Differ.* **17,** 268–277
45. Ho, L. H., Read, S. H., Dorstyn, L., Lambrusco, L., and Kumar, S. (2008) *Oncogene* **27,** 3393–3404
46. Zhang, Y., Padalecki, S. S., Chaudhuri, A. R., De Waal, E., Goins, B. A., Grubbs, B., Ikeno, Y., Richardson, A., Mundy, G. R., and Herman, B. (2007) *Mech. Ageing Dev.* **128,** 213–221
47. Tamm, C., Zhivotovsky, B., and Ceccatelli, S. (2008) *Apoptosis* **13,** 354–363
48. Madesh, M., Zong, W. X., Hawkins, B. J., Ramasamy, S., Venkatachalam, T., Mukhopadhyay, P., Doonan, P. J., Irrinki, K. M., Rajesh, M., Pacher, P., and Thompson, C. B. (2009) *Mol. Cell. Biol.* **29,** 3099–3112
49. Kumar, S., Kinoshita, M., Noda, M., Copeland, N. G., and Jenkins, N. A. (1994) *Genes Dev.* **8,** 1613–1626
50. Kumar, S., Tomooka, Y., and Noda, M. (1992) *Biochem. Biophys. Res. Commun.* **185,** 1155–1161
51. Lamkanfi, M., Declercq, W., Kalai, M., Saelens, X., and Vandenabeele, P. (2002) *Cell Death Differ.* **9,** 358–361
52. Wang, X., Yang, C., Chai, J., Shi, Y., and Xue, D. (2002) *Science* **298,** 1587–1592
53. Bouchier-Hayes, L. (2010) *J. Cell Mol. Med* **14,** 1212–1224
54. Troy, C. M., Rabacchi, S. A., Hohl, J. B., Angelastro, J. M., Greene, L. A.,

and Shelanski, M. L. (2001) *J. Neurosci.* **21,** 5007–5016
55. Kumar, S. (2009) *Nat. Rev. Cancer* **9,** 897–903
56. Chauvier, D., Lecoeur, H., Langonné, A., Borgne-Sanchez, A., Mariani, J., Martinou, J. C., Rebouillat, D., and Jacotot, E. (2005) *Apoptosis* **10,** 1243–1259
57. Troy, C. M., Rabacchi, S. A., Friedman, W. J., Frappier, T. F., Brown, K., and Shelanski, M. L. (2000) *J. Neurosci.* **20,** 1386–1392
58. Schweizer, A., Briand, C., and Grutter, M. G. (2003) *J. Biol. Chem.* **278,** 42441–42447
59. Zheng, T. S., Hunot, S., Kuida, K., Momoi, T., Srinivasan, A., Nicholson, D. W., Lazebnik, Y., and Flavell, R. A. (2000) *Nat. Med.* **6,** 1241–1247
60. Takai, Y., Matikainen, T., Jurisicova, A., Kim, M. R., Trbovich, A. M., Fujita, E., Nakagawa, T., Lemmers, B., Flavell, R. A., Hakem, R., Momoi, T., Yuan, J., Tilly, J. L., and Perez, G. I. (2007) *Apoptosis* **12,** 791–800
61. Troy, C. M., Stefanis, L., Greene, L. A., and Shelanski, M. L. (1997) *J. Neurosci.* **17,** 1911–1918
62. Levine, B., and Yuan, J. (2005) *J. Clin. Invest.* **115,** 2679–2688
63. Yu, L., Strandberg, L., and Lenardo, M. J. (2008) *Autophagy* **4,** 567–573
64. Shimizu, S., Kanaseki, T., Mizushima, N., Mizuta, T., Arakawa-Kobayashi, S., Thompson, C. B., and Tsujimoto, Y. (2004) *Nat. Cell Biol.* **6,** 1221–1228
65. Yu, L., Alva, A., Su, H., Dutt, P., Freundt, E., Welsh, S., Baehrecke, E. H., and Lenardo, M. J. (2004) *Science* **304,** 1500–1502
66. Kuwana, T., and Newmeyer, D. D. (2003) *Curr. Opin. Cell Biol.* **15,** 691–699